

Review on Recent Developments in Collimators of Single Photon Emission Computed Tomography Imaging

Parvaneh Darkhor, Jalil Pirayesh Islamian * 

Departments of Medical Physics, Faculty of Medicine, Tabriz University of Medical Sciences, Tabriz, Iran

*Corresponding Author: Jalil Pirayesh Islamian
Email: pirayeshj@gmail.com

Received: 10 February 2020 / Accepted: 08 March 2020

Abstract

In Single Photon Emission Computed Tomography (SPECT), collimator selection, optimization, and also geometric calibration have a major impact on the acquired image quality and also on an accurate detectability and diagnosis. The collimator optimization phenomena consider some parameters such as field of view, resolution, sensitivity, resolution at depth, septal thickness and penetration for a specific application task. While the parallel hole collimator is usually used in SPECT and planar imaging but due to the limited solid angle covered by the collimator, the system sensitivity and resolution were highly reduced. Meanwhile, other types of collimators such as pin-hole, multi-pin-hole, slant and slit-slat collimators were introduced with a trade-off between sensitivity and resolution. This article reviews improvements on collimators also by considering the geometry and geometric calibration methods for improving the image quality in single photon emission computed tomography.

Keywords: Collimator; Resolution; Image Quality; Single Photon Emission Computed Tomography; Sensitivity.

1. Introduction

The image quality and also accuracy of data acquisition in nuclear medicine imaging are affected by various components of the imaging chain consisting of collimator and gantry design, physical properties of detector, reconstruction algorithms, attenuation and scatter compensation approaches [1-5]. Employing an appropriate collimator with a certain radiopharmaceutical is a critical factor to create a high quality image [6, 7]. In this context, recent SPECT hardware, including the collimator and detector, was combined with reconstruction software to improve system performance for both human and small animal molecular imaging [8, 9]. There has been much improvement in collimator geometry and also reconstruction algorithms [7, 8, 10-12]. Parallel hole collimator is routinely used to planar and SPECT imaging [13-17]. An array of holes separated by thin walls (septa), which are fabricated by employing heavy elements, e.g. lead or tungsten, constitutes the geometry of a collimator. The septal penetration depends on several factors, including septal thickness, hole length, and the energy of the incident gamma rays. Ideally, it is assumed that all the photons striking the septa were absorbed (Figure 1). Thus, only the photons that travel within the acceptance angle of collimator holes would pass through and could be detected [18].

Collimation geometry has a critical role in providing a detailed image from a target organ and so controls noise, resolution, and sensitivity of the imaging system. The collimator optimization phenomena consider some parameters such as field of view, resolution, sensitivity, resolution at depth, septal thickness and penetration for a specific application task [14, 7, 8, 11]. Here, improvement of the collimators in SPECT is reviewed by brief overview on collimator geometry and configuration, including parallel hole, pin-hole, and slant hole collimators.

2. Classification of the Collimators

Resolution and sensitivity are two main performance factors in collimator designing [19]. The spatial resolution is often measured as: (1) the

minimum distinguishable distance of two line sources or (2) the Full Width at Half Maximum (FWHM) from the Point Spread Function (PSF) [20-22]. Meanwhile, geometry of a collimator determines spatial resolution of a SPECT system [14, 7, 23, 24].

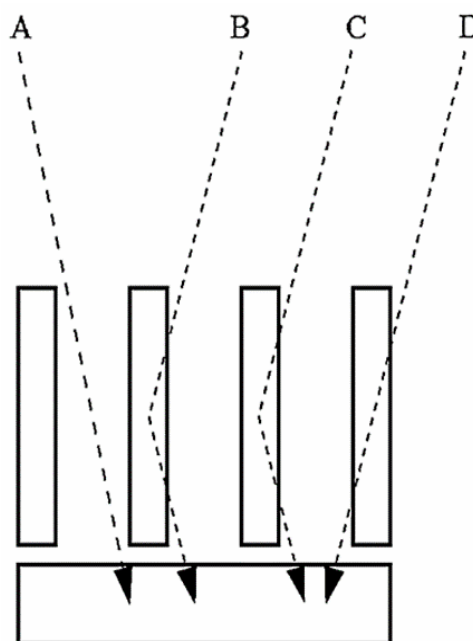


Figure 1. The types of photon interactions in a collimator: geometrically collimated photon (A), a scattered photon (B), a lead X-ray fluorescence photon (C), and a penetrated photon (D) [18]

Collimator aperture size plays a critical role in system resolution and so sensitivity. The smaller holes lead to the better resolution versus lower sensitivity. In 2014, Park *et al.* compared detection efficiency of collimators with hexagonal, 12-gonal, and 24-gonal hole geometries with the diameters of 0.54, 1, 1.4 cm, respectively [25]. They found a better detection efficiency for the 12-gonal and 24-gonal systems compared to the hexagonal. According to the lattice structure of the hole patterns, collimators are categorized as parallel hole, pin-hole, convergent, divergent, fan or cone beam collimators [21]. Space limitation, spatial resolution and sensitivity are determinant in collimator selection for a particular imaging task [14, 11]. An appropriate collimator needs to be selected for a specific imaging application, for instance a fan or cone beam collimator for brain imaging, a pin-hole collimator for thyroid, and parallel-hole collimator as generally used in SPECT and planar imaging [7, 20, 26].

In a study by Park *et al.* in 2016, a novel Ultrashort Cone-Beam (USCB) collimator (Figure 2) was proposed for early identification of Parkinson's disease [27].

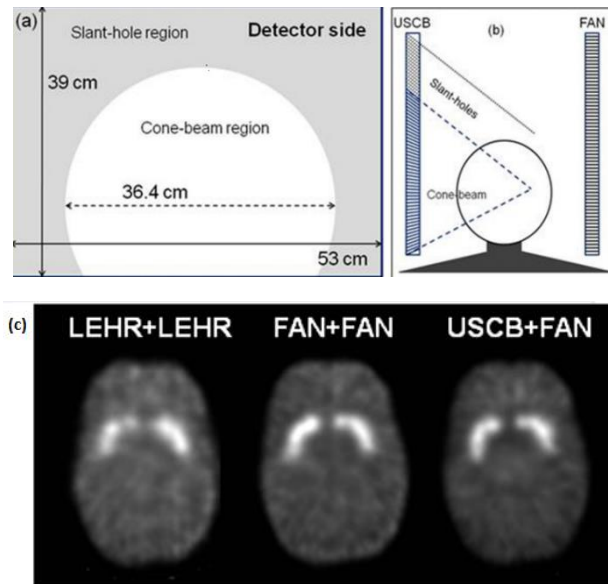


Figure 2. Schematic view of an Ultrashort Cone-Beam (USCB) collimator, (a) detector side of the collimator, (b) the collimator configuration for a brain SPECT acquisition combining USCB and FAN collimators, (c) Transverse slice through reconstructed images of the striatal phantom with a 5:1 striatal/background concentration of ^{99m}Tc [27]

Meanwhile, growing interest in improving image quality and diagnostic accuracy had also led to introduce a new collimator geometry in cardiac SPECT imaging [28-33]. The new IQ SPECT equipped with multifocal collimators provides a better sensitivity (4-fold) and contrast-to-noise ratio than the common parallel hole collimator for cardiac studies. In this configuration, the collimator consists of the holes which focusing array centrally and near parallel at peripherals. Furthermore, it was proposed that IQ SPECT can help in shorter acquisition times so without loss of diagnostic accuracy may improve patient comfort and streamline departmental efficiency [34].

Diverging collimators were proposed by Park *et al.* in 2014 to enhance the performance of industrial SPECT systems for flow visualization in industrial reactors [35]. The diverging collimator not only provides extensive areas compared to a parallel hole collimator, but also reduces the system size of an

industrial SPECT system to investigation and visualization of flows in industrial flow reactors.

2.1. Parallel-Hole Collimators

A parallel hole collimator involves numerous holes in small honeycomb straight closely packed configurations on a plate of dense material (an alloy of lead and antimony). According to the design type, parallel hole collimators have about 4000-46000 apertures [9, 36-38]. The length, diameter, wall thickness and forming material of the holes can play an important role in the clarity of images so that the beams, which straightly reach the hole from the organ, are allowed to pass by the collimator, and the others emitted with some oblique angles are eliminated [37, 39]. A parallel hole collimator has a finite length and hole size and, therefore, the passed photons are from the area enclosed by a cone whose vertex is interaction site of the photon on the crystal. In this case, the number of scattered photons increases with the distance of the source from the collimator encompassing more area and, therefore, spatial resolution decreases [37]. However, point source sensitivity of the collimator is identical everywhere in the FOV, but resolution depends on object to the collimator distance [3, 8].

The sensitivity and resolution measurements of a Parallel Hole collimator (PH) with hexagonal holes were given by Equations 1 and 2, respectively [16].

$$\text{sensitivity}_{(PH)} = \frac{\sqrt{3}}{8\pi} \frac{d^2}{a_{eff}^2} \frac{d^2}{(d+t)^2} \quad (1)$$

$$\text{Resolution}_{(PH)} = d \frac{a+h}{a_{eff}} \quad (2)$$

Where d , t , and h are hole diameter, septal thickness, and source-to-detector distance, respectively. $a_{eff} = a - 2/\mu$ is the physical hole length and considers penetration effect, where a and μ are collimator thickness and attenuation coefficient ($1/\mu = 0.37$ mm for ^{99m}Tc source and the lead collimator), respectively. The system spatial resolution (R_{sys}) is related to the intrinsic resolution (R_{intr}) and collimator resolution (R_{col}) by [9]:

$$R_{sys} = \sqrt{R_{col}^2 + R_{intr}^2} \quad (3)$$

In a study in 2016, Li *et al.* proposed a new design of Multi-Resolution Multi-Sensitivity (MRMS) collimator which was based on a parallel hole collimator [39]. Originally, their study introduced a double collimating design which collimates gamma rays by double layers of the parallel hole collimator. The advantages of multiple resolution/sensitivity trade-offs can be obtained through changing the layers thickness ratio.

The tradeoff between the spatial resolution and the geometric efficiency is a compromise on image quality so that to achieve a reasonable spatial resolution, the geometric efficiency of parallel hole collimator must inevitably be very low [40], and a proper source-to-collimator distances is also needed [40]. Finally, a field of view about 40 cm for a parallel hole collimator is defined in the modern gamma cameras [21, 41].

2.2. Pin-Hole Collimators

The pin-hole collimation has been introduced to compensate the low photon detection efficiency of parallel-hole systems and to improve the image contrast [11, 17]. The collimator consists of a single hole drilled into a lead sheet [6, 20]. A pin-hole with knife edge geometry is the most popular pin-hole opening design (Figure 3) [14]. It was shown that an aperture with a diameter of 4-6 mm

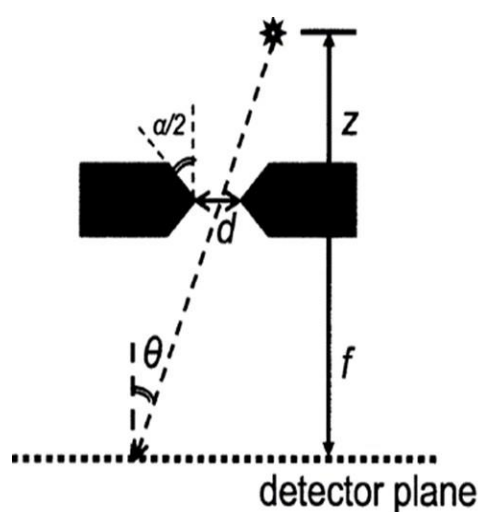


Figure 3. A knife edge aperture design for pin-hole collimator. (a: acceptance angle, d: physical pin-hole aperture opening diameter, f: focal distance, z: distance from object to the pin-hole aperture, and θ : incidence angle) [14]

provides a better spatial resolution [7, 42]. Multi pin-hole collimators have focused peripheral apertures to the FOV [43, 44]. SPECT imaging with pin-hole includes small organs such as thyroid, parathyroid glands, knee joints, breast, and also small animal's physiological imaging [7, 14, 45-47].

In knee joints imaging, pin-hole leads to an improved spatial resolution by magnifying small structures of different radiotracer uptakes. Also pinholes with some better penetration characteristics are a suitable option for isotopes with higher photopeak energy (e.g. ^{111}In) [48].

In small animal imaging, single pin-hole collimation is often used for acquiring image magnification and high spatial resolution. However, due to its low sensitivity, multi-pin-hole collimator is an alternative instead. Overlapping pin-hole projections create multiplexing artifacts in reconstructed images. However, helical acquisitions can provide sufficient data sampling and suppress the artifact. In a study by Ukon *et al.* in 2016, the optimal helical acquisition parameters in small animal whole body SPECT utilizing five-pin-hole collimator had been proposed [49].

In comparison with a parallel-hole collimator, a pin-hole collimator has a smaller Field of View (FOV) and so preferred in focal uptake imaging [7, 20]. Due to the small FOV, pin-hole collimation has insufficient axially coverage of an entire animal for small animal imaging and also suffers from the low detection efficiency [13, 14, 45]. A multi-pin-hole collimator allows increasing FOV, sensitivity and detection efficiency without reducing the spatial resolution [13, 14, 45].

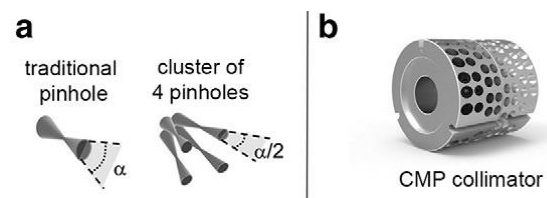


Figure 4. (a) Traditional pin-hole with an opening angle α and cluster of 4 pin-holes with approximately the same field of view and opening angle $\alpha/2$. (b) Clustered Multi Pin-hole (CMP) collimator optimized for imaging high energy gamma rays [50]

In addition to pin-holes, which were used as SPECT collimators, the Clustered Multi-Pin-hole (CMP) collimation provides simultaneous sub-millimeter imaging in SPECT and PET, either due to the narrower opening angles (Figure 4), penetration of the photons decreases through the pin-hole edges [50]. However, overlap of the projections through the pin-holes is a primary limitation in a multi-pin-hole collimation, but detector coverage of the collimator is rather efficient by several projections through the multi-pin-holes [13, 14, 45].

2.3. Slant Hole Collimators

Different types of slant hole collimators have been established in the last decades. Variations of the collimation geometries are included: Slit-Slat (SS), Multi-Slit Slat (MSS), Rotating Slant (RS), Four Segment Slant Hole (FSSH), Rotating Multi-Segment Slant Hole (RMSSH) and Rotating Multi-Segment Variable Slant Angle (RMSVSH) collimator [28].

The slit-slat collimation combines parallel hole and pin-hole properties and allows a better detection efficiency than a multi-pin-hole collimator [51-54]. The slits are oriented parallel to the rotation axis and form a long knife-edges configuration (Figure 5). Slit-slat collimator provides a parallel collimation in the axial direction through its parallel slats. Two motions are necessary when data acquisition with a slat collimator: a rotation in axial and another in its own central direction [9]. The running along the axial direction provides the collimation like a pin-hole in the transverse plane. Slit-slat collimators were proposed in small animal imaging as well as in human cardiac and brain imaging [55]. The slat collimators with a large solid angle and cylindrical FOV can cover whole animal with a square gamma detector (Figure 6). Drawback of the collimator is its limited axial resolution which causes a non-isotropic performance of the Point Spread Function (PSF) [11].

In a study by Kamali Asl *et al.* in 2005, the effect of a slit-slat collimator dimension on MTF, efficiency, and spatial resolution for 511 Kev photons had been evaluated. They demonstrated a better image quality using a slit slant collimator than a parallel hole collimator. Furthermore, because of the related higher efficiency and so shorter scan time, the patient motion artifact can be reduced [23, 29]. In 2009, Accorsi *et*

al., compared performance of the pin-hole and slit-slat collimators for circular and polygonal orbits. Their results showed that a very tight polygonal orbit provides sensitivity advantage only in the case of pin-hole collimator [56].

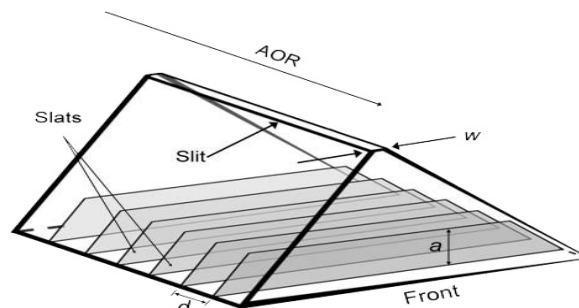


Figure 5. Schematic configuration of a slit-slat collimator. The slit is parallel to the Axis of Rotation (AOR). Normal to slats are also parallel to AOR. (a : slit height; d : slit spacing; and w : slit width) [6]

By comparing multi-pin-hole and multi-slit slit-slat collimators, the first geometry has shown a better reconstructed image uniformity and trans-axial resolution, while the multi-slit gave better axial resolution [6, 7, 57]. Rotating Slant hole collimator (RS) is another alternative to the parallel hole collimation. In comparison to a parallel hole, with a fixed spatial resolution, RS gives improved detection efficiency by a factor of five. Indeed, a better trade-off was provided with this collimation geometry between spatial resolution and detection efficiency [58]. In contrast to the slant collimator, the RS collimator suffers from higher background radiation [59, 11]. Because of the slant geometry, the RSH SPECT has much smaller FOV than parallel hole SPECT and so it is appropriate for detecting small breast lesions [14, 16, 43].

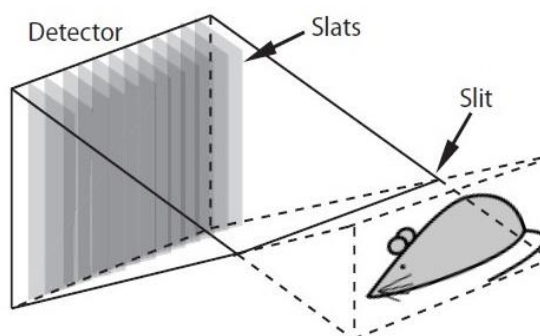


Figure 6. Illustration of FOVs with a slit-slat collimator that covers an entire mouse [52]

In the 1980's, Change *et al.* utilized a four segment RSH collimator for cardiac SPECT imaging and acquired simultaneously four projections from different views. The results showed an increased detection efficiency and also improved noise properties so that they suggested RSH collimator as a good alternative for cardiac imaging [14, 33, 43, 60, 61]. A multi-segment slant hole collimator has been introduced by dividing parallel hole collimator into multiple segments and then slanting the holes towards a Common Volume of View (CVOV) [14]. On the other hand, a segment in Rotating Multi-Segment Slant Hole (RMSSH) collimator consists of parallel holes slanted at a fixed angle [16, 62]. This configuration provides a complete set of projection data by rotating ability around the RMSSH collimator. Similar to the other type of slant collimators, RMSSH collimator has much higher detection efficiency than conventional SPECT with a parallel hole collimator. As well with the RMSSH collimator, it can be image of the breast at a closer distance [14, 16]. It must be mentioned that in RMSSH geometry, collimator holes are slanted parallel but in RMSVSH collimator each segment has made by collimator holes with the slant angle (outer slant angle) to the center (inner slant angle). This collimator forms 1D divergent beam geometry with an enlarged Common Volume of View (CVOV) [63]. Wang has studied applications of two high sensitivity and high-resolution SPECT imaging techniques with unconventional collimator geometries, including RMSSH and pin-hole in small animal imaging [14]. He revealed that via pin-hole collimation, high resolution images (less than 1 mm) can be achieved.

2.4. Collimator Optimization Procedure

Collimator optimization procedure is achieved by evaluating the parameters which play an effective role in sensitivity and spatial resolution of the collimator. For a pin-hole collimator the parameters include collimator length (t), source to collimator distance (d), effective radius of the pin-hole (r_e), radius of the aperture (r), and angle between the pin-hole and Y-axis (α). For a parallel hole collimator, the parameters are t , d , r , septal thickness (s), collimator to detector distance (c), and effective thickness of the collimator (t_e). These parameters are also the same for converging and diverging hole collimators in addition

to two extra parameters: f (focal point) and α (slant angle of the septa). However, the optimization process for RMSSH collimator is more complicated. Hence, a large number of collimator parameters such as septal thickness, hole length, hole shape, slant angle, and also the number of the segments should be considered to the optimization [23].

2.5. Geometric Calibration of Collimator

Geometric calibration is determining of geometric parameters of an imaging system [14, 15]. Accurate geometric calibration and proper reconstruction algorithm improve quantitative accuracy of the final images [14, 15, 21].

An optimal calibration method mainly depends on the scanner geometry. Busemann-Sokole proposed a calibration method for parallel and slant hole collimators [51]. This calibration procedure measures a plate containing 16 point sources at two different positions. While for fan beam geometry, decreasing the distance between the experimental measurement and analytic positions of a point source is optimal calibration method that firstly was presented by Gullberg *et al.* [64]. In 2015, Mao *et al.* introduced a 2-step calibration method for the segmented slant hole collimator [15]. By this method, the reconstructed image acquires with any visible distortion. Geometric calibration method for pin-hole and cone beam CT is mathematically equivalent. So the results from pin-hole calibration can be applied to cone beam CT as well. Beque *et al.* used three point sources with a specific position to provide an optimal pin-hole SPECT calibration [65]. Consequently, it should be noted that the calibration of SPECT systems with the sophisticated collimators are more complicated than the conventional parallel hole systems [15].

3. Conclusion

The collimator choice for a specific imaging task is based on several factors, including the required intrinsic resolution, sensitivity, and also spatial resolution. The slant collimator with a much larger solid angle potentially increases the low detection sensitivity from a thin crystal than a parallel hole. Both RMSSH and pin-hole collimators with a similar philosophy provide an enhanced tradeoff between the

detection efficiency and the spatial resolution in exchange for a reduced FOV. As well, the multiplexing effect in multi-pin-hole and multi-slit-slat collimators can lead to an increased sensitivity and SNR at the resulted images.

References

- 1- Van Audenhaege, Karen *et al.* "Review of SPECT collimator selection, optimization, and fabrication for clinical and preclinical imaging," *Medical physics*, vol. 42, no. 8, pp. 4796-813, 2015.
- 2- M. Ljungberg, "Absolute quantification of SPECT studies." *Seminars in Nuclear Medicine*, vol. 48, Issue 4, pp. 348-358, 2018.
- 3- A. Sadremontaz and Z. Telikani, "Evaluation of the performance of parallel-hole collimator for high resolution small animal SPECT: A Monte Carlo study," *Iranian J Nucl Med*, vol. 24, no. 2, pp. 136-143, 2016.
- 4- A. Azarm, J. P. Islamian, B. Mahmoudian, and E. Gharepapagh, "The Effect of Parallel-hole Collimator Material on Image and Functional Parameters in SPECT Imaging: A SIMIND Monte Carlo Study," *World J Nucl Med*, vol. 14, no. 3, p. 160-164, 2015.
- 5- B. F. Hutton, K. Erlandsson, and K. Thielemans, "Advances in clinical molecular imaging instrumentation," *Clinical and Translational Imaging*, vol. 6, no. 1, pp. 31-45, 2018.
- 6- S. D. Metzler, R. Accorsi, J. R. Novak, A. S. Ayan, and R. J. Jaszczak, "On-axis sensitivity and resolution of a slit-slat collimator," *J Nucl Med*, vol. 47, no. 11, pp. 1884-1890, 2006.
- 7- J. P. Islamian, A. Azazrm, B. Mahmoudian, and E. Gharapapagh, "Advances in Pinhole and Multi-Pinhole Collimators For Single Photon Emission Computed Tomography Imaging," *World J Nucl Med*, vol. 14, no. 1, pp. 3-9, 2015.
- 8- P. J. Slomka, T. Pan, D. S. Berman, and G. Germano, "Advances in SPECT and PET Hardware," *Prog Cardiovasc Dis*, vol. 57, no. 6, pp. 566-578, 2015.
- 9- K. Van Audenhaege, R. Van Holen, S. Vandenberghe, C. Vanhove, S. D. Metzler, and S. C. Moore, "Review of SPECT collimator selection, optimization, and fabrication for clinical and preclinical imaging," *Med phys*, vol. 42, no. 8, pp. 4796-4813, 2015.
- 10- G. J. Hademenos, "Optimization of a pinhole collimator in a SPECT scintillating fiber detector system: A Monte Carlo analysis," *Radiat Phys Chem*. vol. 43, pp.383-392,1994.
- 11- N. Dehestani, S. Sarkar, M. R. Ay, M. Sadeghi, and M. Shafaei, "Comparative Assessment of Rotating Slit and Parallel Hole Collimator Performance in GE DST-Xli Gamma Camera: A Monte Carlo Study," in *4th European Conference of the International Federation for Medical and Biological Engineering*, 2009, pp. 1062-1065.
- 12- A. Kamali-Asl, S. Sarkar, M. Shahriari, and H. Agha-Hosseini, "Slit slit collimator optimization with respect to MTF," *Appl Radiat Isot*, vol. 62, no. 3, pp. 461-468, 2005.
- 13- M. F. Smith, "Recent advances in cardiac SPECT instrumentation and system design," *Curr Cardiol Repp*, vol. 15, no. 8, pp. 1-11, 2013.
- 14- Y. Wang, "Development and applications of high-sensitivity and high-resolution fully 3D SPECT imaging techniques using two different collimator designs," 2014. <https://search.proquest.com/docview/305170496?accountid=41307>. Accessed 20 Nov 2019.
- 15- Y. Mao, Z. Yu, and G. L. Zeng, "Geometric calibration and image reconstruction for a segmented slant-hole stationary cardiac SPECT system," *J Nucl Med Technol*, vol. 43, no. 2, pp. 103-112, 2015.
- 16- J. Xu, C. Liu, Y. Wang, E. C. Frey, and B. M. Tsui, "Quantitative rotating multisegment slant-hole SPECT mammography with attenuation and collimator-detector response compensation," *IEEE Trans Med Imaging*, vol. 26, no. 7, pp. 906-916, 2007.
- 17- J. D. Bowen *et al.*, "Design and performance evaluation of a 20-aperture multipinhole collimator for myocardial perfusion imaging applications," *Phys Med Biol*, vol. 58, no. 20, pp. 7209-7226, 2013.
- 18- A. O. Sohlberg and M. T. Kajaste, "Fast Monte Carlo-simulator with full collimator and detector response modelling for SPECT," *Ann Nucl Med*, vol. 26, no. 1, pp. 92-98, 2012.
- 19- H. Mahani, A. Kamali-Asl, and M.R. Ay, "How gamma camera's head-tilts affect image quality of a nuclear scintigram?," *Front Biomed Technol*, vol. 1, no. 4, pp. 265-270, 2015.
- 20- L. Chen, B.M. Tsui, G.S.P. Mok, "Design and evaluation of two multi-pinhole collimators for brain SPECT," *Ann Nucl Med*, vol. 31, pp. 636-48, 2017.
- 21- H. Ye, "Development and Implementation of Fully Three-dimensional Iterative Reconstruction Approaches in Spect with Parallel, Fan-and Cone-beam Collimators," *ProQuest*, 2008. <https://search.proquest.com/docview/304366011?accountid=41307>. Accessed 20 Jun 2019.
- 22- P. D. Esser, P. O. Alderson, R. J. Mitnick, and J. J. Arliss, "Angled-collimator SPECT (A-SPECT): an improved approach to cranial single photon emission tomography," *J Nucl Med*, vol. 25, no. 7, pp. 805-809,

- 1984.
- 23- R.M. Capote, N. Matela, R.C. Conceicao, P. Almeida, "Optimization of convergent collimators for pixelated SPECT systems," *Med Phys*, vol. 40, issue 6, pp. 062501, 2013.
- 24- J. P. Islamian, M. T. B. Toossi, M. Momennezhad, S. R. Zakavi, R. Sadeghi, and M. Ljungberg, "Monte carlo study of the effect of collimator thickness on T^{99m} source response in single photon emission computed tomography," *World J Nucl Med*, vol. 11, no. 2, pp. 70-74, 2012.
- 25- J. G. Park, S.-H. Jung, J. B. Kim, J. Moon, M. C. Han, and C. H. Kim, "Development of advanced industrial SPECT system with 12-gonal diverging-collimator," *Appl Radiat Isot*, vol. 89, pp. 159-166, 2014.
- 26- N. Bhusal, J. Dey, J. Xu, K. Kalluri, A. Konik, J.M. Mukherjee, P.H. Pretorius, "Performance analysis of a high-sensitivity multi-pinhole cardiac SPECT system with hemi-ellipsoid detectors," *Med Phys*, vol. 46, no 1, pp. 116-126, 2019.
- 27- M.-A. Park *et al.*, "Introduction of a novel ultrahigh sensitivity collimator for brain SPECT imaging," *Med Phys*, vol. 43, no. 8, pp. 4734-4741, 2016.
- 28- G. Bal, E.V.R. Dibella, G. Gullberg, G.L. Zeng, "Cardiac imaging using a four-segment slant-hole collimator," *IEEE trans nucl sci*, vol. 53, pp. 2619-27, 2006.
- 29- Erlandson K, Kacperski K, Gramberg D, Hutton BF. "Performance evaluation of D-SPECT: a novel SPECT system for nuclear cardiology," *Phys Med Biol*, vol. 54, pp.2635-49, 2009.
- 30- Liu C, Xu J, Tsui B. "Development and evaluation of rotating multi-segment variable-angle slant-hole SPECT," *J Nucl Med*, vol. 48, 161P, 2007.
- 31- Mao Y, Yu Z, Zeng GL, "Geometric calibration and image reconstruction for a segmented slant-hole stationary cardiac SPECT system," *J Nucl Med Technol*, vol. 43, pp. 103-112 2015.
- 32- Smith MF. "Recent advances in cardiac SPECT instrumentation and system design," *Curr cardiolo rep*, vol. 15, pp. 1-11, 2013.
- 33- C. Liu, J. Xu, B.M. Tsui, "Myocardial perfusion SPECT using a rotating multi-segment slant-hole collimator," *Med phys*, vol. 37, pp.1610-8, 2010.
- 34- F. Caobelli, J. T. Thackeray, A. Soffientini, F. M. Bengel, C. Pizzocaro, and U. P. Guerra, "Feasibility of one-eighth time gated myocardial perfusion SPECT functional imaging using IQ-SPECT," *Eur J Nucl Med Mol Imaging*, vol. 42, no. 12, pp. 1920-1928, 2015.
- 35- J. G. Park, S.-H. Jung, J. B. Kim, J. Moon, Y. S. Yeom, and C. H. Kim, "Performance evaluation of advanced industrial SPECT system with diverging collimator," *Appl Radiat Isot*, vol. 94, pp. 125-130, 2014.
- 36- B. Wang, "3D Scintillation Positioning Method in a Breast-specific Gamma Camera," 2015. <http://urn.kb.se/resolve?urn=urn:nbn:se:kth:diva-177180>. Accessed 28 Feb 2019.
- 37- A. K. Pandey, S. K. Sharma, P. K. Sellam Karunanithi, C. Bal, and R. Kumar, "Characterization of parallel-hole collimator using Monte Carlo Simulation," *IJNM*, vol. 30, no. 2, p. 128, 2015.
- 38- Y. J. Lee and H. J. Kim, "Comparison of a newly-designed stack-up collimator with conventional parallel-hole collimators in pre-clinical CZT gamma camera systems: a Monte Carlo simulation study," *J Korean Phys Soc*, vol. 65, no. 7, pp. 1149-1158, 2014.
- 39- Y. Li, P. Xiao, X. Zhu, and Q. Xie, "Multi-resolution multi-sensitivity design for parallel-hole SPECT collimators," *Phys Med Bio*, vol. 61, no. 14, p. 5390, 2016.
- 40- L. Zhou, K. Vunckx, and J. Nuyts, "Parallel hole and rotating slat collimators: Comparative study using digital contrast phantoms," *IEEE Trans Nucl Sc*, vol. 60, no. 5, pp. 3282-3289, 2013.
- 41- C. Liu, J. Xu, B.M. Tsui, "Myocardial perfusion SPECT using a rotating multi-segment slant-hole collimator," *Medical physics*, vol. 37, no. 4, pp.1610-1618, 2010.
- 42- A. Seret and F. Bleeser, "Intrinsic uniformity requirements for pinhole SPECT," *J Nucl Med Technol*, vol. 34, no. 1, pp. 43-47, 2006.
- 43- G.S. Mok, *et al.*, "Development and validation of a Monte Carlo simulation tool for multi-pinhole SPECT," *Mol Imaging Biol*, vol. 12, no.3, pp. 295-304, 2010.
- 44- Y. Higaki, *et al.*, "Appropriate collimators in a small animal SPECT scanner with CZT detector," *Ann Nucl Med*, vol. 27, no. 3, pp. 271-278, 2013.
- 45- C. Si, G.S. Mok, L. Chen, B.M. Tsui, "Design and evaluation of an multipinhole collimator for high-performance clinical and preclinical imaging," *Nucl Med Commun*, vol. 37, no.3, pp. 313-21, 2016.
- 46- Y. Higaki, M. Kobayashi, T. Uehara, H. Hanaoka, Y. Arano, and K. Kawai, "Appropriate collimators in a small animal SPECT scanner with CZT detector," *Ann Nucl Med*, vol. 27, no. 3, pp. 271-278, 2013.
- 47- M. M. Khalil, J. L. Tremoleda, T. B. Bayomy, and W. Gsell, "Molecular SPECT imaging: an overview," *Int J Mol Imaging*, vol. 2011, 2011, Art. no. 796025.
- 48- K. Van Audenhaege, S. Vandenberghe, K. Deprez, B.

- Vandeghinste, and R. Van Hoken, "Design and simulation of a full-ring multi-lofthole collimator for brain SPECT," *Phys Med Biol*, vol. 58, no. 18, p. 6317, 2013.
- 49- N. Ukon, N. Kubo, M. Ishikawa, S. Zhao, N. Tamaki, and Y. Kuge, "Optimization of helical acquisition parameters to preserve uniformity of mouse whole body using multipinhole collimator in single-photon emission computed tomography," *Res Phys*, vol. 6, pp. 659-663, 2016.
- 50- F. van der Have, O. Ivashchenko, M. C. Goorden, R. M. Ramakers, and F. J. Beekman, "High-resolution clustered pinhole 131 Iodine SPECT imaging in mice," *Nucl Med Bio*, vol. 43, no. 8, pp. 506-511, 2016.
- 51- E. Busemann-Sokole, "Measurement of collimator hole angulation and camera head tilt for slant and parallel hole collimators used in SPECT," *Journal of nuclear medicine: official publication, Society of Nuclear Medicine*, vol. 28, no. 10, pp. 1592-1598, 1987.
- 52- L. Cao and J. Peter, "Slit-slat collimator equipped gamma camera for whole-mouse SPECT-CT imaging," *IEEE Transactions on Nuclear Science*, vol. 59, no. 3, pp. 530-536, 2012.
- 53- S. D. Metzler, R. Accorsi, A. S. Ayan, and R. J. Jaszczak, "Slit-slat and multi-slit-slat collimator design and experimentally acquired phantom images from a rotating prototype," *IEEE transactions on nuclear science*, vol. 57, no. 1, pp. 125-134, 2010.
- 54- S. D. Metzler, R. Accorsi, J. R. Novak, A. S. Ayan, and R. J. Jaszczak, "On-axis sensitivity and resolution of a slit-slat collimator," *Journal of Nuclear Medicine*, vol. 47, no. 11, pp. 1884-1890, 2006.
- 55- D. Kau and S. D. Metzler, "Finding optimized conditions of slit-slat and multislit-slat collimation for breast imaging," *IEEE Trans Nucl Sci*, vol. 59, no. 1, pp. 62-69, 2012.
- 56- R. Accorsi, A. S. Ayan, and S. D. Metzler, "Comparison of circular and polygonal planar orbits for pinhole and slit-slat SPECT," *IEEE Trans Nucl Sci*, vol. 56, no. 3, p. 694, 2009.
- 57- D. Salvado *et al.*, "Collimator design for a clinical brain SPECT/MRI insert," *EJNMMI physics*, vol. 1, p. A21, 2014.
- 58- F. Boisson, V. Bekaert, D. Brasse, "Determination of optimal collimation parameters for a rotating slat collimator system: a system matrix method using ML-EM," *Phys Med Biol*, vol. 61, no. 6, pp.2302-18, 2016.
- 59- F. Boisson, V. Bekaert, Z. El Bitar, J. Wurtz, J. Steibel, and D. Brasse, "Characterization of a rotating slat collimator system dedicated to small animal imaging," *Phys Med Biol*, vol. 56, no. 5, p. 1471, 2011.
- 60- R. Van Hoken, S. Vandenberghe, S. Staelens, and I. Lemahieu, "Comparing planar image quality of rotating slat and parallel hole collimation: influence of system modeling," *Phys Med Biol*, vol. 53, no. 7, p. 1989, 2008.
- 61- G. Bal, R. Clackdoyle, D. J. Kadrmas, G. L. Zeng, and P. Christian, "Evaluating rotating slant-hole SPECT with respect to parallel hole SPECT," in *Nuclear Science Symposium Conference Record*, 2000 IEEE, 2000, vol. 3, pp. 22/67-22/71 vol. 3: IEEE.
- 62- C. Liu, J. Xu, and B. Tsui, "Development and evaluation of rotating multi-segment variable-angle slant-hole SPECT," *J Nucl Med*, vol. 48, no. supplement 2, pp. 161, 2007.
- 63- J. Xu, C. Liu, and B. Tsui, "Completeness conditions in rotating multi-segment variable slant angle SPECT technique," in *Society of Nuclear Medicine Annual Meeting Abstracts*, 2007, vol. 48, no. Supplement 2, pp. 424P: Soc Nuclear Med.
- 64- G.T. Gullberg, B.M. Tsui, C. Crawford, E.R. Edgerton, "Estimation of geometrical parameters for fan beam tomography," *Phys Med Biol*, vol. 32, pp.1581-1594, 1987.
- 65- D. Bequé, J. Nuyts, P. Suetens, and G. Bormans, "Optimization of geometrical calibration in pinhole SPECT," *IEEE Trans Med Imaging*, vol. 24, no. 2, pp. 180-190, 2005.